Mathematical modelling of the anthocyanin adsorption was carried out by using four kinetic equations of three kinetic models: formal kinetics, of the pseudo-first and pseudo-second order. It was found out that the equation of the pseudo-second order best describes the experimental kinetic curves of anthocyanin adsorption from Red Cabbage extracts on bentonite. Thus theoretical values of the equilibrium adsorption of anthocyanins from Red Cabbage extracts on bentonite are closest to the experimentally obtained values of equilibrium adsorption with using the model of pseudo-second order. For the same model, all the experimental kinetic curves had a linear determination coefficient above 0.99.

Keywords: adsorption, kinetics, anthocyanins, bentonite.

Матеріал надійшов 11.01.2016

УДК 544.723.212

T. Tatarchuk, N. Paliychuk

ADSORPTION OF METHYLENE BLUE ONTO $CoFe_2O_4$ SPINEL FERRITE NANOPARTICLES

The influence of the synthesis method (chemical co-precipitation, sol-gel method) on the structure and morphology of the $CoFe_2O_4$ nanoparticles was considered and characterized by X-ray powder diffraction (XRD), Fourier infrared spectroscopy (FT-IR), and scanning electron microscopy (SEM). Crystallite sizes of $CoFe_2O_4$ synthesized by zol-gel and co-precipitation methods range from 9 to 42 nm. The adsorption property of spinel ferrites in relation to organic dye methylene blue was described. The influence of initial dye concentration at the adsorption capacity of magnetic spinel nanosorbents was considered. The adsorption of these dyes is well described by kinetic models of Langmuir. The adsorption isotherms show that the adsorption efficiency of $CoFe_2O_4$ nanoparticles, synthesized by co-precipitation method at 800 °C, is the highest because it has a larger degree of structure inversion.

Keywords: adsorption, spinel, ferrite, $CoFe_2O_4$, adsorbent, methylene blue, dye, adsorption isotherms.

Introduction

Spinel ferrites are intensively studied for their good magnetic property and stable chemical property. They shows typical ferromagnetic property at room temperature and it is wildly use as magnetic carrier in adsorbent to realize magnetic separation. Applications of ferrites of nanometer size have prompted the development of several widely used methods, including sol-gel techniques, reverse micelles, co-precipitation, citrate precursor techniques and other, for the fabrication of spinel ferrite nanoparticles [1–16].

Spinel compounds have the general formula AB_2O_4, in which the A-site is tetrahedrally coordinated and generally occupied by divalent cations, such as Ni and Co. The B-site is octahedrally coordinated and occupied by trivalent cations like Fe and Cr. Spinels are attractive subjects for continuous scientific interest and have been deeply investigated in materials sciences because of their physico-chemical properties [17]. The physical characteristics of the spinel adsorbents, such as, surface area, porosity, size distribution, density and surface charge have high influence in the adsorption process. As a result, there has been a great interest in developing new adsorbent materials with diverse compositions, properties and functionalities [17].

Many physical and chemical methods have been used for the dye removal from wastewaters. Traditionally used methods include coagulation, sedimentation and activated sludge, etc. More advanced methods include ozonation, membrane separation, electrochemical and ultrasonic techniques, photocatalysis [3], adsorption, etc. [4]. Magnetic separation technology is a fast and easy method for separating magnetic adsorbents from an aqueous solution. In recent years, magnetic separation technology, combined with the adsorption process, has been widely used for dye removal from wastewaters [1; 4; 9–13].

The removal of methylene blue (MB) from wastewaters is an environmental issue and has launched the extensive research efforts in this regard. It is a heterocyclic aromatic compound, which is heavily used in the textile industry, and it is present in the effluents of wastewaters coming from other industries. The acute exposure to methylene blue dye may cause some harmful effects such as increased heart rate, shock, vomiting, jaundice, and tissue necrosis in humans [14; 18]. Methylene blue has been selected for the present study. MB is common dye that has been studied as a model compound for organic contaminants. The structure of MB contains a phenothiazine with a dimethyl amine on each side (Table 1).

Table 1. **Structure and characteristics of methylene blue dye**

Name	Methylene blue
Formula	$C_{16}H_{18}ClN_3S$
Molecular weight	319.85 g/mole
λ_{max}	662 nm
Chemical structure	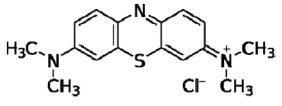

This study has investigated the efficiency of spinel-type oxides nanoparticles $CoFe_2O_4$, synthesized by co-precipitation method and zol-gel method, as an adsorbent for removal of MB from an aqueous solution.

Materials and methods

1. Sample preparations

1.1. Synthesis of nanocrystalline $CoFe_2O_4$ by chemical co-precipitation method

All chemicals were of analytical grade and were used without further purification: $Co(NO_3)_2 \cdot 6H_2O$, $Fe(NO_3)_3 \cdot 9H_2O$, NaOH. The starting materials $Fe(NO_3)_2 \cdot 9H_2O$ and $Co(NO_3)_2 \cdot 6H_2O$ were dissolved in 700 ml of distilled water by intensive stirring, accordingly a homogeneous solution was obtained, and then NaOH was added to the solution until the pH 11.5. After the completion of the reaction, the solid product washed several times with deionized water. The final product was dried oven at 100 °C for 6 h, then was calcined at 800 °C for 2 h. Black powders were obtained and characterized as nanocrystalline $CoFe_2O_4$ ferrites. The reaction may be written as follows:

$$Co(NO_3)_2 \cdot 6H_2O + 2\,Fe(NO_3)_3 \cdot 9H_2O + $$
$$+ H_2O \rightarrow Co^{2+} + 2Fe^{3+} + 8NO_3^- + 25H_2O$$
$$Co^{2+} + 2Fe^{3+} + 8NaOH \xrightarrow{80^o C} Co(OH)_2\downarrow + $$
$$+ 2Fe(OH)_3\downarrow + 8Na^+$$
$$Co(OH)_2 + 2Fe(OH)_3 \xrightarrow{800^o C} CoFe_2O_4 + 4H_2O.$$

1.2. Synthesis of nanocrystalline $CoFe_2O_4$ by citrate sol-gel method

The chemicals used for the preparation of the samples were ferric nitrate ($Fe(NO_3)_3 \cdot 9H_2O$, Mw = 403.8597 g/mole), cobalt nitrate ($Co(NO_3)_2 \cdot 6H_2O$, Mw = 290.943 g/mole), citric acid ($C_6H_8O_7$, Mw = 192.06 g/mole) and ammonia solution (25 %). $Co(NO_3)_2 \cdot 6H_2O$, $Fe(NO_3)_3 \cdot 9H_2O$ were dissolved in 200 ml distilled water under constant stirring to get homogeneous solution. Citric acid was dissolved in 100 ml distilled water and added to metal citrates solution in molar ratio of 1:1. Then the resulting solution was stirred at 20 °C with addition ammonia solution to get pH = 7.0. After having been stirred, the sol was being heated at 100 °C until the brown gel was formed. This gel combusted and fluffy product was obtained. The general nitrate-citrate combustion reaction may be written as follows:

$$Co(NO_3)_2 \cdot 6H_2O + 2Fe(NO_3)_3 \cdot 9H_2O + 3C_6H_8O_7 \rightarrow$$
$$\rightarrow CoFe_2O_4 + 4N_2\uparrow + 18CO_2\uparrow + 36H_2O.$$

2. Characterizations

X-ray diffraction (XRD) pattern of the samples was taken using X-ray diffractometer DRON-3 with $Cu_{K\alpha}$ radiation of wavelength $\lambda = 0.15406$ nm at 30 kV and 15 mA. The X-ray diffraction patterns were recorded in the angular range $15° \leq 2\theta \leq 65°$ with a step size of 0.05°. XRD pattern was analyzed by Rietveld method by the software FullProf.

Fourier transmission infrared (FTIR) spectrum of the powders was recorded in the range 4000–350 cm^{-1} by means of an Alpha-P Fourier-transform infrared spectrometer (Bruker) in ATR mode on diamond window with 256 scans at 6 cm^{-1} resolution. Each spectrum was the average of six ones.

The Brunauer-Emmett-Teller (BET) surface area (m^2/g) was determined from nitrogen adsorption/desorption isotherms at a temperature of 77 K using a Quantachrome NOVA surface area analyzer.

The morphological studies were carried out by scanning electron microscopy using JEOL JSM-T220A scanning microscope (Japan) with an accelerating voltage of 20 kV.

3. Adsorption studies

After we ascertain the pure phase $CoFe_2O_4$ spinel ferrites, a series adsorption experiments were carried out. Effect of the concentration of MB was investigated by repeating experiments with different initial concentrations (10, 25, 50 and 150 $mg \cdot L^{-1}$) of MB. A stock solution of 150 mg/L of methylene blue was prepared.

The quantity of the powder added was 0.5 g in each flask and the all the flasks were shaken at room temperature. After a specified time, the solid and liquid were separated by magnet and the absorption spectrums of the solutions were studied on the spectrophotometer at the λ_{max} of the dye which is 662 nm. A standard curve, which was used to convert absorbance data into concentrations for equilibrium studies, was drawn to calculate the concentration of each experiment.

The amount of adsorbed MB ($mg \cdot g^{-1}$) was calculated based on a mass balance equation as given below:

$$q_e = \frac{(C_o - C_e) \cdot V}{m},$$

where q_e is the equilibrium adsorption capacity per gram dry weight of the adsorbent, $mg \cdot g^{-1}$; C_0 is the initial concentration of MB in the solution, mg/L; C_e is the final or equilibrium concentration of MB in the solution, mg/L; V is the volume of the solution, L and m is the dry weight of the $CoFe_2O_4$, g [1].

Results and discussion

1. Characterizations of synthesized materials

The sol-gel and precipitated fine particles were characterized by XRD for structural determination and estimation of crystallite size. The diffraction patterns of the samples shows the formation of the single-phase spinel structure with the Fd3m space group. X-ray diffraction (XRD) patterns of the samples are shown in Fig. 1.

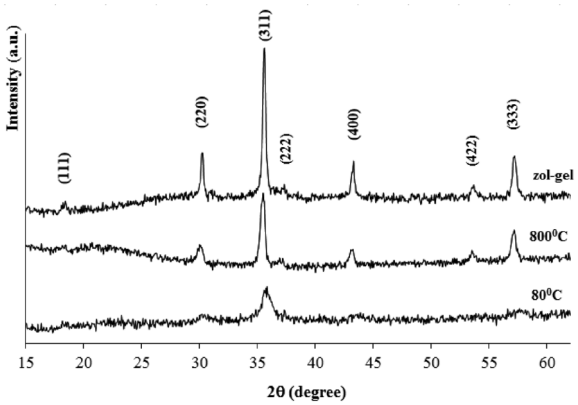

Fig. 1. X-ray diffraction patterns of the synthesized cobalt ferrites at different conditions

The average crystallite size of $CoFe_2O_4$ nanoparticles was estimated using Scherrer formula:

$$D_C = \frac{0{,}94\lambda}{\beta_{1/2}\cos\theta},$$

where D_C is the crystallite size, nm; $\beta_{1/2}$ is the peak width at half-maximum intensity, degrees; θ is the Bragg angle, and λ is the wavelength of the X-ray radiation ($\lambda = 0.15406$ nm). To determine the crystallite sizes, the most intense diffraction line (311) were used. The average crystallite sizes D are calculated from the characteristics of the (311) XRD-peaks through the Scherrer formula are shown in Table 2.

Table 2. **Crystallite size and lattice parameter of $CoFe_2O_4$, synthesized by zol-gel and co-precipitation methods**

Sample	Crystallite size, nm	Lattice parameter, nm	ρ_{XRD}, g/cm^3	Surface area, m^2/g
$CoFe_2O_4$-80°	9	0.829 ± 0.002	5.48	143
$CoFe_2O_4$-800°	28	0.8349 ± 0.0003	5.36	10
$CoFe_2O_4$-zol-gel	42	0.8377 ± 0.001	5.30	12

In spinel-type oxides the process of cation inversion is a very common phenomenon, being possible any distribution between a normal and an inverse spinel: $\left(A^{2+}_{1-\delta}B^{3+}_{\delta}\right)_A\left[A^{2+}_{\delta}B^{3+}_{2-\delta}\right]_B\left(O^{2-}_4\right)_O$ (A – divalent cations Co^{2+}, B – trivalent cations Fe^{3+}, δ – inversion parameter representing the fraction of A cations in octahedral sites). The cation distribution in tetrahedral and octahedral interstitial sites were estimated using the Rietveld refinement of the occupancy values. For $CoFe_2O_4$-zol-gel sample cation distribution is described $\left(Co^{2+}_{0,2}Fe^{3+}_{0,8}\right)_A\left[Co^{2+}_{0,8}Fe^{3+}_{1,2}\right]_B\left(O^{2-}_4\right)_O$ (δ = 0.8), while for $CoFe_2O_4$-800° sample cation distribution is described $\left(Fe^{3+}\right)_A\left[Co^{2+}Fe^{3+}\right]_B\left(O^{2-}_4\right)_O$ (δ = 1).

Fig. 2 shows the FTIR spectra of $CoFe_2O_4$, synthesized by zol-gel and co-precipitation methods. Two characteristic peaks observed at around 350–375 cm^{-1} and 540–565 cm^{-1} corresponds to octahedral-metal stretching and to intrinsic stretching vibrations of the metal at the tetrahedral site respectively, which is indicative of the formation of spinel ferrite structure. The peaks observed at around 3400 and 1500 cm^{-1} are ascribed due to the stretching modes and H–O–H bending vibration of the free or absorbed water molecules on the surface of the ferrites [2].

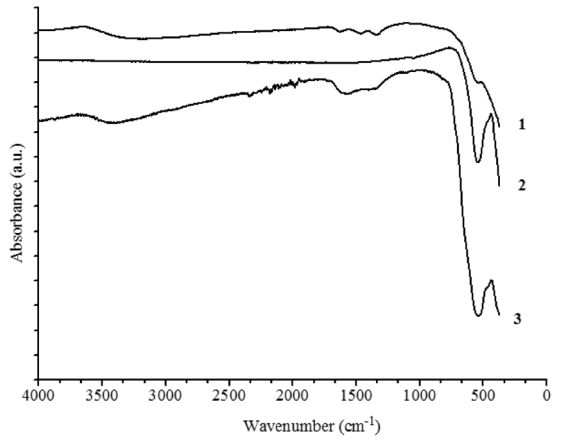

Fig. 2. Infrared spectra of $CoFe_2O_4$ nanoparticles, synthesized by co-precipitation method (*1* – at 80 °C, *2* – at 800 °C) and zol-gel method (*3*)

The morphologies of obtained sample have been characterized by scanning electron microscopy. SEM images reveal the agglomerated structure of the synthesized material (Fig. 3). We assume that the small spheroidal crystals correspond to the magnetic $CoFe_2O_4$ spinel. Agglomerates have size in the range 50–500 nm and are bound to each other creating large structures. $CoFe_2O_4$ nanoparticles are seen as dense aggregates.

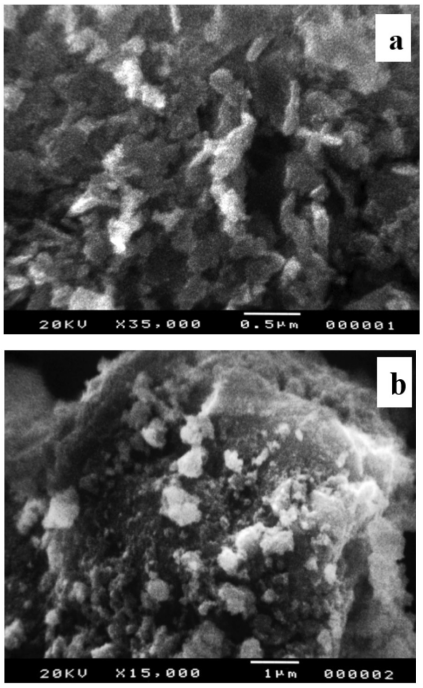

Fig. 3. SEM images of $CoFe_2O_4$ nanoparticles: *a* – synthesized by co-precipitation method at 800 °C; *b* – synthesized by zol-gel method

2. Adsorption of methylene blue dye

The quantity of the dye that could be adsorbed $CoFe_2O_4$ nanoparticles surface is a function of concentration, which could be explained by the adsorption isotherms. In the present study, the Langmuir and Freundlich isotherms are tested for methylene blue dye adsorption.

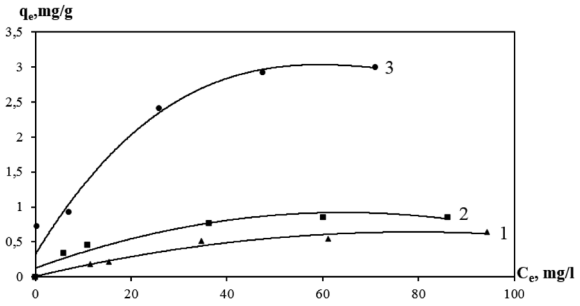

Fig. 4. Adsorption isotherms of MB onto $CoFe_2O_4$ nanoparticles, synthesized by co-precipitation method (*1* – at 80 °C; *3* – at 800 °C) and zol-gel method (*2*) (experimental conditions: T = 20 °C, pH = 7.0; adsorbent dose 500 mg)

From Fig. 4, the adsorption capacity of MB onto $CoFe_2O_4$, synthesized by zol-gel method is 0.86 mg/g, while the adsorption capacity for $CoFe_2O_4$ nanoparticles, synthesized by co-precipitation method at 80 °C and 800 °C, are 0.63 and 3.0 mg/g respectively. The adsorption of MB is fast at the initial stage, and then, it becomes slower near the

equilibrium. It would be for that a large number of vacant surface sites are available for adsorption during the initial stage of the treatment time, and after a lapse of time, the remaining vacant surface sites are difficult to be occupied due to repulsive forces between MB adsorbed on the surface of $CoFe_2O_4$ ferrites and solution phase. It is clear that the adsorption process is highly dependent on initial concentration of solution. The higher adsorption capacity of $CoFe_2O_4$ nanoparticles, synthesized by co-precipitation method at 800 °C, may be due to the smaller crystallite size and distribution of cations between A- and B-sites in spinel lattice.

The Langmuir adsorption isotherm assumes that adsorption takes place at specific homogeneous sites within the adsorbent. The Langmuir isotherm can be written in this form:

$$\frac{C_e}{q_e} = \frac{1}{q_{\max} K_L} + \frac{C_e}{q_{\max}},$$

where C_e (mg/L) is the equilibrium concentration, q_{max} (mg/g) is the amount of adsorbate adsorbed per unit mass of adsorbate (q_{max} is the maximum adsorption capacity of the adsorbate by the adsorbent) and K_L is the Langmuir adsorption constants related to the rate of adsorption [6].

When c_e/q_e was plotted against c_e, a straight line with slope $1/q_{max}$ was obtained indicating that the adsorption of methylene blue onto $CoFe_2O_4$ nanoparticles follows the Langmuir isotherm (Fig. 5). The Langmuir constants K_L calculated from this isotherm and their values are listed in Table 3. Another important parameter, R_L called the separation factor or the equilibrium parameter that is determined from the relation:

$$R_L = \frac{1}{1 + K_L C_e},$$

where K_L is the Langmuir constant (l/mg) and C_e (mg/L) is the highest dye concentration. The value of R_L indicates the type of the isotherm to be either unfavorable ($R_L > 1$), linear ($R_L = 1$), favorable ($0 < R_L < 1$), or irreversible ($R_L = 0$). R_L values for methylene blue adsorption onto $CoFe_2O_4$ nanoparticles were calculated and found to be less than 1 and greater than zero indicating the favorable adsorption of MB (Table 3).

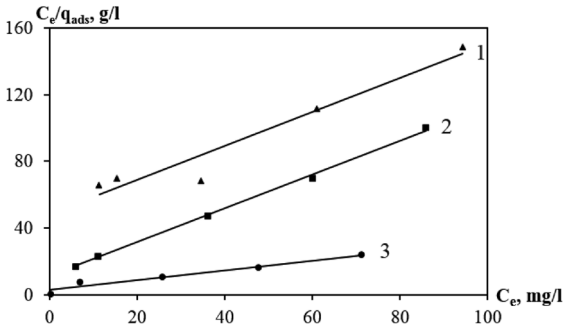

Fig. 5. Langmuir isotherms for $CoFe_2O_4$ nanoparticles, synthesized by zol-gel and co-precipitation methods, for MB dye adsorption: *1* – co-precipitation, 80 °C; *2* – zol-gel; *3* – co-precipitation, 800 °C

The Freundlich isotherm is an empirical equation employed to describe the heterogeneous systems. The Freundlich equation is as follows:

$$\log q_e = \log K_F + \frac{1}{n} \log C_e,$$

where q_e is the amount adsorbed at equilibrium (mg/g) and C_e is the equilibrium concentration of methylene blue. n and K_F are Freundlich constants, n giving an indication of how favorable the adsorption process and K_F (mg/g $(L/mg)^{1/n}$) is the adsorption capacity of the adsorbent. The slope 1/n ranging between 0 and 1 is a measure of the adsorption intensity or the surface heterogeneity, becoming more heterogeneous as its value gets closer to 0. The plot of log q_e versus log C_e (Fig. 6) gives straight lines with slope 1/n reflecting that the adsorption of methylene blue also follows the Freundlich isotherm. Accordingly, Freundlich constants (K_F and n) were calculated and listed in Table 3.

Table 3. **Langmuir and Freundlich parameters for the adsorption of methylene blue on $CoFe_2O_4$ at 298 K**

Isotherms	Parameters	$CoFe_2O_4$ (sol-gel)	$CoFe_2O_4$ (80 °C)	$CoFe_2O_4$ (800 °C)
Langmuir	q_{max} (mg/g)	0.988	0.979	3.374
	K_L (L/mg)	0.088	0.021	0.110
	R_L	0.111	0.32711	0.095
	R^2	0.9983	0.9546	0.9376
Freundlich	K_F (mg/g(L/mg)$^{1/n}$	0.188	0.041	0.968
	n	2.75	1.58	4.06
	R^2	0.9666	0.9225	0.813

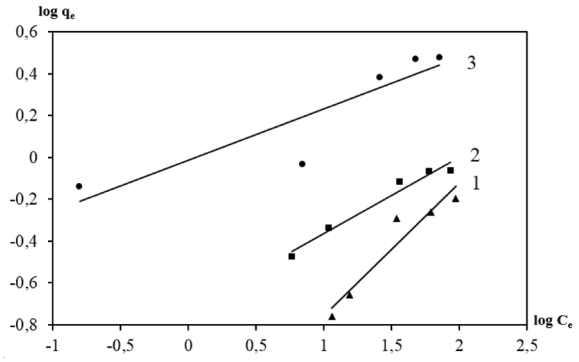

Fig. 6. Freundlich isotherms for $CoFe_2O_4$ nanoparticles, synthesized by zol-gel and co-precipitation methods, for MB dye adsorption: *1* – co-precipitation, 80 °C; *2* – zol-gel; *3* – co-precipitation, 800 °C

Higher value for K_L indicates higher affinity for adsorbate and the values of the empirical parameter 1/n lie between $0.1 < 1/n < 1$, indicating favorable adsorption. Freundlich constants are shown in Table 1. The values of 1/n are in the range of $0.1 < 1/n < 1$, indicating the favorable removal conditions. However, the correlation coefficients ($R^2 = 0.9666$; 0.9225; 0.813) reflects that the experimental data do not fit with the Freundlich model well. The comparison of correlation coefficient (R^2) of the linearized form of both equations indicates that the Langmuir model yields a better fit for the experimental equilibrium adsorption data than the Freundlich model.

For $CoFe_2O_4$ obtained by co-precipitation method at 80 °C the adsorption values for MB is the lowest. This can be explained by the presence of a large number of surface OH-groups that slows down adsorption of basic dye MB. The adsorption capacity $CoFe_2O_4$ obtained by co-precipitation method and annealed at 800 °C is higher than that of $CoFe_2O_4$, obtained by sol-gel method. Since the discrepancy of S_{BET} is not very large for ferrite $CoFe_2O_4$-800 and $CoFe_2O_4$-zol-gel, the discrepancy of adsorption capacities may mainly cause by the differences of their structures. Cations distribution (A- and B-sites) of spinel ferrite might be the most important factor to decide their adsorption capacity. Hence, we can believe that the larger the degree of inversion, the greater the charge on the active centers of the spinel lattice and higher adsorption capacity. So, ferrite $CoFe_2O_4$-800 has larger the degree of structure inversion.

Conclusion

In this paper, $CoFe_2O_4$ powders were synthesized by two chemical methods, that is, co-precipitation and citrate sol-gel method. The X-ray diffraction patterns reveal the formation of single-phase cubic spinel structure for all the samples. The crystallite size of the product was found in nanometric dimensions using a line profile fitting of the XRD pattern. The infrared spectral analysis of the prepared material confirms the formation of the spinel ferrite phase. Adsorption isotherm studies clearly indicated that the Langmuir equation showed a better fit for adsorption of MB dye by $CoFe_2O_4$, implying a monolayer/homogeneous binding surface. The sample $CoFe_2O_4$-800 shows the largest adsorption capacity. In our study the adsorption properties of Co ferrite are dependent on the distribution of the cations between A- and B-sites.

References

1. Decoration of multi-walled carbon nanotubes (MWCNTs) with different ferrite nanoparticles and its use as an adsorbent / A. Farghali, M. Bahgat, W. Elrouby, M. Khedr // Journal of Nanostructure in Chemistry. – 2013. – Vol. 3, № 50. – P. 1–12.
2. Marechal M. L. Decolouration of chlorotriazine reactive azo dyes with H_2O_2/UV / M. L. Marechal, Y. M. Slokar, T. Taufer // Dyes Pigments. – 1997. – Vol. 33, Is. 4. – P. 281–298.
3. Factorial experimental design of orange II photocatalytic discoloration processs / J. Fernandez, J. Kiwi, C. Lizama [et al.] // J. Photochem.Photobiol. A. – 2002. – Vol. 151. – P. 213–219.
4. Removal of dyes from colored textile wastewater by orange peel adsorbent: equilibrium and kinetic studies / M. Arami, N. Y. Limaee, N. M. Mahmoodi, N. S. Tabrizi // J. Colloid Interface Sci. – 2005. – Vol. 288. – P. 371–376.
5. Equilibrium and kinetic studies on acid dye Acid Red 88 adsorption by magnetic $ZnFe_2O_4$ spinel ferrite nanoparticles / W. Konicki, D. Sibera, E. Mijowska [et al.] // J. of Colloid and Interface Sci. – 2013. – Vol. 152. – P. 398.
6. Panneerselvam P. Magnetic nanoparticle (Fe_3O_4) impregnated onto tea waste for the removal of nickel(II) from aqueous solution / P. Panneerselvam, N. Morad, K. A. Tan // J. Hazard. Mater. – 2011. – Vol. 186. – P. 160–168.
7. A facile thermolysis route to monodisperse ferrite nanocrystals / N. Bao, L. Shen, Y. Wang [et al.] // J. Am. Chem. Soc. – 2007. – Vol. 129. – P. 12374–12375.
8. Synthesis of ferrites obtained from heavy metal solutions using wet method / Y. Ji, P. Juan, L. Kaicheng [et al.] // J. Hazard. Mater. – 2007. – Vol. 143. – P. 379–385.
9. Ismail B. Adsorption of methylene blue onto spinel magnesium aluminate nanoparticles: adsorption isotherms, kinetic and thermodynamic studies / B. Ismail, S. T. Hussain, S. Akram // Chem. Eng. J. – 2013. – Vol. 219. – P. 395–402.
10. Masoud S. N. A simple route to synthesize nanocrystalline nickel ferrite ($NiFe_2O_4$) in the presence of octanoic acid as a surfactant / S. N. Masoud, D. Fatemeh, M. Tahmineh // Polyhedron. – 2009. – Vol. 28. – P. 1455–1458.
11. Adsorption capability for Congo red on nanocrystalline MFe_2O_4 (M = Mn, Fe, Co, Ni) spinel ferrites / L. Wang, J. Li, Y. Wang [et al.] // Chemical Engineering Journal. – 2012. – Vol. 72. – P. 181–182.
12. Adsorption and magnetic removal of neutral red dye from aqueous solution using Fe_3O_4 hollow nanospheres / M. Iram, C. Guo, Y. Guan [et al.] // J. Hazard. Mater. – 2010. – Vol. 181. – P. 1039–1050.
13. Magnetic and high rate adsorption properties of porous $Mn1-xZnxFe_2O_4$ ($0 \le x \le 0.8$) adsorbents / X. Y. Hou, J. Feng,

X. H. Liu [et al.] // J. Colloid Interface Sci. – 2011. – Vol. 353. – P. 524–529.
14. Ai L. Removal of methylene blue from aqueous solution by montmorillonite/$CoFe_2O_4$ composite with magnetic separation performance / L. Ai, Y. Zhou, J. Jiang // Desalination. – 2011. – Vol. 266. – P. 72–77.
15. Zhou L. Magnetic dendritic materials for highly efficient adsorption of dyes and drugs / L. Zhou, C. Gao, W. Xu // ACS Appl. Mater. Interface. – 2010. – Vol. 2. – P. 1483–1491.
16. Arsenite and arsenate adsorptionon coprecipitated bimetal oxide magnetic nanomaterials: $MnFe_2O_4$ and $CoFe_2O_4$ / S. X. Zhang, H. Y. Niu, Y. Q. Cai [et al.] // Chem. Eng. J. – 2010. – Vol. 158. – P. 599–607.
17. Khosravi I. Characterization and evaluation catalytic efficiency of $NiFe_2O_4$ nanospinel in removal of reactive dye from aqueous solution / I. Khosravi, M. Eftekhar // Powder Technology. – 2013. – Vol. 147. – P. 250.
18. Ismail B. Adsorption of methylene blue onto spinel magnesium aluminate nanoparticles: Adsorption isotherms, kinetic and thermodynamic studies / B. Ismail, S. T. Hussain, S. Akram // Chemical Engineering Journal. – 2013. – Vol. 395. – P. 219.

Татарчук Т. Р., Палійчук Н. Д.

АДСОРБЦІЯ МЕТИЛЕНОВОГО СИНЬОГО НА НАНОЧАСТИНКАХ ШПІНЕЛЬНОГО ФЕРИТУ $CoFe_2O_4$

Описано вплив методу отримання (хімічного співосадження, цитратного золь-гель методу автогоріння) на структуру і будову наночастинок $CoFe_2O_4$ на основі даних Х-променевого аналізу, ІЧ-спектроскопії, сканувальної електронної мікроскопії (СЕМ). Розмір кристалітів $CoFe_2O_4$, синтезованих золь-гель методом і методом хімічного співосадження, перебуває в межах від 9 до 42 нм. Охарактеризовано адсорбційні властивості шпінельних феритів відносно органічного барвника метиленового синього. Досліджено вплив початкової концентрації метиленового синього на адсорбційну здатність магнітних шпінельних наночастинок. Показано, що дані адсорбції краще описуються кінетичною моделлю Ленгмюра. Адсорбційні ізотерми показують, що адсорбційна здатність наночастинок $CoFe_2O_4$, синтезованих методом хімічного співосадження і відпалених за температури 800 °С, є найвищою і пояснюється впливом ступеня оберненості шпінельної структури.

Ключові слова: адсорбція, шпінель, ферит, $CoFe_2O_4$, адсорбент, метиленовий синій, барвник, ізотерма адсорбції.

Матеріал надійшов 20.01.2016